

## Low temperature synthesis of alpha alumina platelets and acicular mullite in MgO-Al<sub>2</sub>O<sub>3</sub>-SiO<sub>2</sub> system

M. A. Zalapa-Garibay<sup>1, 2</sup>, A. Arizmendi-Moraquecho<sup>2</sup>, S. Y. Reyes-López<sup>\*3</sup>

<sup>1</sup>Instituto de Ingeniería y Tecnología, Universidad Autónoma de Ciudad Juárez, Av. del Charro 450, Partido Romero C.P. 32310.

<sup>2</sup>Centro de Investigación de Materiales Avanzados, Alianza Norte 202. Parque de Investigación e Innovación Tecnológica, Alianza Norte, Apodaca, Nuevo León, México. C.P. 66600

<sup>3</sup>Instituto de Ciencias Biomédicas, Universidad Autónoma de Ciudad Juárez, Envolvente del PRONAF y Estocolmo s/n, Ciudad Juárez, Chih., México C.P. 32300.

received August 27, 2018; received in revised form February 28, 2019; accepted March 15, 2019

### Abstract

The refractory materials are more reliable and less expensive, this research is based on materials like alumina and mullite because it offers a very high refractoriness. In the present study an acicular mullite and  $\alpha$ -alumina platelets were synthesized by using a synthesis of chemicals related to raw materials SiO<sub>2</sub> 45 wt%-Al<sub>2</sub>O<sub>3</sub> 45 wt% - MgO 10 wt%. The  $\alpha$ -alumina platelets and acicular mullite were obtained in a reduced processing time and temperature, compare to conventional methods, such as sol-gel method, microwave sintering, chemical synthesis, combustion synthesis and lip casting and sintered. The composition, thermal analysis and micro structure evolution were followed by X-ray diffraction, differential thermal analysis and scanning electron microscopy (SEM). The synthesis of chemicals method based on Pechini process was successfully to synthesize  $\alpha$ -alumina platelets and acicular mullite. All the precursor powders used have an amorphous structure with submicron particle size. The effect of MgO in the formation of  $\alpha$ -alumina platelets and acicular mullite at low temperature was found. The  $\alpha$ -alumina platelets and acicular mullite was detected after heating at 800 °C and the dissolution  $\alpha$ -alumina platelets for the formation of secondary mullite is around 1000 °C. It was observed that at 1400 °C it's crystallized type III of secondary mullite. The behavior of the evolution of the phases and compact solid samples from oxides was made.

*Keywords:* Mullite, alumina, microstructure.

### I. Introduction

Currently, ceramics, refractory materials, glass-ceramics materials and composite materials based on the MgO-Al<sub>2</sub>O<sub>3</sub>-SiO<sub>2</sub> system has received increasing value among the materials for the new fields of engineering. The products manufactured with these materials have a coefficient of low thermal expansion, a high mechanical resistance and a high thermal and chemical resistance<sup>1</sup>. The morphology and stoichiometry of mullite can obviously be influenced by the starting materials and the processing technique. However, it is known, for example, that the stoichiometric mullite 3Al<sub>2</sub>O<sub>3</sub>·2SiO<sub>2</sub> is only formed from oxide precursors at high temperatures, while the non-stoichiometric mullite 2Al<sub>2</sub>O<sub>3</sub>·SiO<sub>2</sub> is derived only from the melt-derived systems. Subsequently, the unstable spinel precursor phase of mullite is transformed into orthorhombic mullite at 1075 °C. Furthermore, the chemical nature of precursory phases can modify the temperature of mullite formation. In porcelain bodies and glass ceramics, primary mullite can form on the surface of kaolinite relicts

that in turn serves as a seed for the crystallization of the secondary mullite needles as alkali diffuses out of feldspar at higher temperatures. As the temperature increases, the grain growth from liquid phase overlaps the dissolution of mullite grains and a bimodal microstructure develops, with an increasing fraction of large tabular grains (acicular mullite)<sup>2,3</sup>. Tertiary mullite has been reported in aluminous porcelains precipitating out of alumina-rich liquid. The starting compositions, and especially the alumina/silica ratio, determine the evolution of mullite crystals growth. Furthermore, the mullitization reaction process is accomplished at lower temperatures if the proportion of alumina in the sample is above the stoichiometric composition of mullite. On the other hand, if the alumina content is too high, the excess alumina might undergo structural rearrangements and give rise to the formation of  $\alpha$ -alumina<sup>2,3</sup>.

Alumina is an advanced material with microelectronic and structural applications, as well as in the technology for thermonuclear fusion reactors. Alumina is an important technical ceramic, extensively used in microelectronics, catalysis, refractories, abrasives and structural applications. Specifically, high quality corundum polycrystalline

\* Corresponding author: [simon.reyes@uacj.mx](mailto:simon.reyes@uacj.mx)

materials are used as electronic substrates and as bearings in watches and in various high precision devices<sup>4</sup>. The  $\alpha$ - $\text{Al}_2\text{O}_3$  is particularly stable due to the selective position of oxygen sublattice in octahedral sites instead of being in both tetrahedral and octahedral sites as in the case of the metastable phases<sup>5</sup>. Alumina ceramics materials are being considered as a promising candidate for dielectric windows on high frequency heating systems due to its very low dielectric losses at high frequencies and its radiation resistance<sup>6</sup>.

Alpha alumina ( $\alpha$ - $\text{Al}_2\text{O}_3$ ) platelet is a very useful material, which exhibits high hardness, high young's modulus, high strength and chemical resistance. The plate-like shape makes  $\alpha$ - $\text{Al}_2\text{O}_3$  platelets useful as reinforcements in various composites because of the energy dissipation induced by the incorporation of platelets<sup>7</sup>. There are several methods for preparing  $\alpha$ - $\text{Al}_2\text{O}_3$  platelets, for instance, Hill *et al*<sup>8</sup> produced  $\alpha$ - $\text{Al}_2\text{O}_3$  platelets by calcining alumina and aluminum fluoride mixture powder. Unfortunately, fluoride required by these methods is harmful to the environment. Miao and Sorrell<sup>9</sup> obtained  $\alpha$ - $\text{Al}_2\text{O}_3$  platelets by calcining a mixture of natural topaz and zirconia. Hashimoto and Yamaguchi<sup>10</sup> synthesized  $\alpha$ - $\text{Al}_2\text{O}_3$  platelets using Sodium sulfate flux. However, these methods need a calcination temperature as high as 1200 °C and will consume too much energy. Recently, Park *et al.*<sup>11</sup> synthesized  $\alpha$ - $\text{Al}_2\text{O}_3$  platelets using flux method in 2.45 GHz microwave field; Wu *et al.*<sup>12</sup> prepared  $\alpha$ - $\text{Al}_2\text{O}_3$  platelets by laser scanning alumina powders; Wei *et al.*<sup>13</sup> synthesized  $\alpha$ - $\text{Al}_2\text{O}_3$  hexagonal platelets using electrostatic spray assisted chemical vapour deposition. However, these techniques require complicated equipment and high temperatures<sup>14,15–20</sup>. Therefore, continuous efforts are being made to develop new processing routes for high quality alumina or mullite based ceramics. These efforts are partially responsible for recent developments of chemical processing approaches, especially for advanced ceramic applications<sup>15–18,21–23</sup>.

The rate of mullite formation depends on the temperature of the reaction<sup>15–17</sup>. For the reason that mullite powder compacts have poor solid state sinterability<sup>13</sup>, many studies had been dedicated to investigating the effect of adding sintering aids such as MgO, SrO,  $\text{B}_2\text{O}_3$ ,  $\text{TiO}_2$ ,  $\text{CeO}_2$  and  $\text{Y}_2\text{O}_3$ <sup>14–36</sup>. It was reported that MgO addition resulted in the formation of mullite with equiaxed morphology, promoted grain growth and increased the density<sup>23,28</sup>. There are several techniques available for the preparation of alumina and acicular mullite platelets, e. g. sol-gel method, microwave sintering, chemical synthesis, combustion synthesis and slip casting and sintered<sup>2,4,7</sup>. Each method has its own characteristics.

The Pechini method or the polymer precursor method is based on the polymerization of metal citrate using ethylene glycol. A hydrocarboxylic acid, such as citric acid, is used to chelate the cations in an aqueous solution. The addition of a glycol such as ethylene glycol leads to the formation of an ester. The polymerization reaction, promoted by heating the mixture, results in a homogeneous resin in which the metal ions are uniformly distributed throughout the organic matrix. A primary heat treatment in an

oxidizing atmosphere around 250–350 °C produces the so-called precursor powder. This method has advantages such as good homogeneity, good stoichiometric control and good control of particle morphology<sup>29</sup>.

The objective of the study is to obtain the composite, by the Pechini method that allows us to obtain the mullite and alumina at lower temperatures, with specific morphologies as the case of the hexagonal plates for the alumina and acicular forms for the mullite. In addition, to the compact densification (alumina-mullite composite) to observe the behavior in the evolution of the phases under these conditions.

## II. Experimental Procedure

### (1) Synthesis of the alumina and mullite powders

The synthesis of the alumina platelets and the acicular mullite were prepared by the Pechini Method. Aluminum oxide, silicon oxide and magnesium oxide ( $\text{Al}_2\text{O}_3$  45 wt%:  $\text{SiO}_2$  45% wt  $\text{MgO}$  10% wt) were dissolved in 10 ml of hydrofluoric acid. Citric acid was subsequently added during stirring, and then the required amount of propylene glycol was added to the solution and heated to 70 °C for 2 hours in HERATHERMM oven OGS60. Finally the pH was adjusted to 9 with ammonium hydroxide (all the reagents used were purchased with the Sigma Aldrich supplier with <99% trace metal basis). The resulting suspension was dried by the spray drying technique to reduce the synthesis time and obtain homogeneous powders. The resulting powder was calcined in the temperature range of 100 to 1500 °C in a conventional resistance furnace MTI 1700X with oxygen atmosphere to obtain the powders, for a permanence time of 2 hours.

### (2) Synthesis of alumina-mullite composite

For comparative purposes, a composite material of mullite-alumina was made using  $\text{SiO}_2$  silicon oxide ( $d_{50}$  = 3.7  $\mu\text{m}$ , Reachim, Russia),  $\alpha$ - $\text{Al}_2\text{O}_3$  alumina ( $d_{50}$  = 3  $\mu\text{m}$ , Nabalox no 325, Nabaltec AG, Germany) and magnesite (Sigma Aldrich <99% trace metal basis, -325 mesh) in dust. The ratio of  $\alpha$ - $\text{Al}_2\text{O}_3$ :  $\text{SiO}_2$ :  $\text{MgO}$  was maintained at 45 wt%:45 wt%:10 wt%. A first step, the powders were mixed in planetary ball milling at a speed of 700 rpm for 3 hours, Poly (vinyl alcohol) (PVA) was added as an organic binder. Subsequently, samples were made with the help of a hydraulic press applying a uniaxial pressure of 2.5 Pa per 1 minute, using a die of 0.5in diameter. The samples were subjected to a heat treatment at 80 °C for a period of two hours, then the samples were sintered at 1100 °C, 1200 °C, 1300 °C and 1400 °C at a heating rate of 10 K/min for 2 hours, using a muffle furnace model MTI 1700X.

### (3) Characterization

The samples of composite material were dried for 48 h at a temperature of 200 °C in a drying in HERATHERM oven. After this period, the weight did not change in the case of the composite. For thermal treatments, a high temperature MTI 1700X furnace was used, using a heating speed of 10 K/min, with a dwell time of 2 hours and a cooling rate of 10 K/min. The compositional and structural study of the powders and composites obtained by each of the synthesis

methods was carried out by means of the following techniques. The gravimetric thermal analysis (TGA) and the differential scanning calorimetry (DSC), were carried out using a New Castle Instrument Q600 instrument, obtaining the sequence of thermal decomposition in the air, in a temperature range of 100 to 1500 °C, using a heating rate of 10 K/min, with 100 cm<sup>3</sup>/min of air flow. The crystal evolution as a function of temperature was determined by X-ray diffraction (Empyrean, Panalytical with  $\text{CuK}\alpha$  radiation). For the characterization by means of infrared spectrometry, an Alpha Platinum FT-IR (Bruker Optics Inc) series equipment was used to obtain infrared spectra using the ATR technique (with diamond crystal), the spectra were accumulated in 64 scans at 2 cm<sup>-1</sup>. Finally, in the characterization by means of scanning electron microscopy (SEM), a Jeol JSM-6010 microscope was used at 20 kV.

### III. Results and discussion

#### (1) Synthesis of the alumina and Mullite powders

##### (a) Thermal gravimetric Analysis and Differential scanning calorimetry

Fig. 1 shows the behavior of the TGA and DSC analyzes. In TGA of previously heated sample at 200 °C a significant weight loss in a temperature range of 25 °C to 450 °C is seen, weight loss is attributed to water and decomposition of organic compounds of the reactions of Pechini method. In the range of 450 °C to 1050 °C, a weight loss of 10% is observed for the decomposition of  $\text{AlF}_3$  and  $\text{Mg}_2\text{SiO}_4$  to form alumina and Mullite. In the range temperature of 1050 °C to 1350 °C, weight gain is observed, which is indicative of an oxidation reaction of the aluminum<sup>4-10</sup>. Subsequently, between 1350 °C and 1500 °C a slight weight loss is observed due to structural rearrangement of  $\alpha$ - $\text{Al}_2\text{O}_3$  platelets and acicular mullite.

Analysis of Differential Scanning Calorimetry presented in Fig. 1 of previously heated sample at 200 °C, reflecting the decomposition of organic compounds having two endothermic peaks at a temperature of 350 °C and 450 °C, one exothermic peak at 1150 °C corresponding to the crystallization of  $\alpha$ - $\text{Al}_2\text{O}_3$  platelets, and finally, the endothermic peak observed at a temperature of 1400 °C probably represents the dissolution temperature for alumina crystal growth of mullite secondary type III. To observe in detail, the phase transitions, the powders were exposed to a heat treatment at 600 °C. Fig. 1 shows in DSC an endothermic peak at 750 °C, attributed to the formation of  $\alpha$ - $\text{Al}_2\text{O}_3$  and primary mullite, ending in tertiary mullite at 1300 °C according with XRD and SEM micrographs<sup>2,3,40-46</sup>. The TGA in Fig. 1 for sample whit heat treatment at 600 °C show a first weight loss from 500 to 800 °C for the absorbed water, a weight loss of ~1% associated with the formation of mullite according whit XRD data.

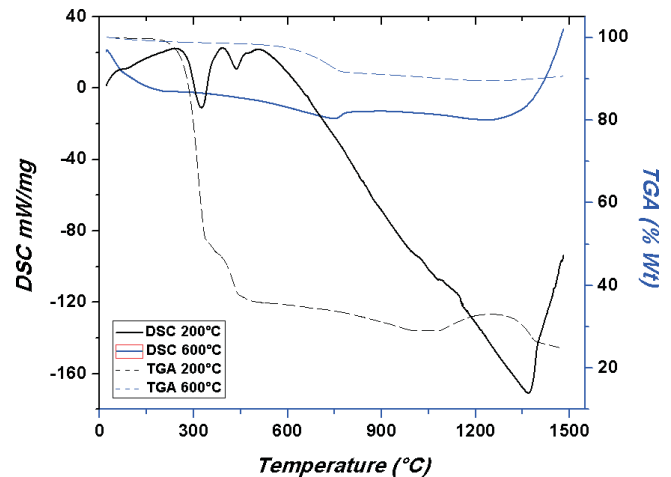


Fig. 1: TGA and DSC curves of experimental obtained by Pechini Method, after heat treatment at 200 °C (black line) and 600 °C (blue line), with rate of 10 K/min up to 1500 °C.

##### (b) X-Ray Diffraction

The results of the XRD analysis of the thermally treated samples are shown in Fig. 2. At 100 °C and 200 °C two phases were identified:  $(\text{NH}_4)_3\text{AlF}_6$  and  $(\text{NH}_4)_2(\text{SiF}_6)$  (ICDD 01-076-0117 and ICDD 01-089-4113 respectively). At 400 °C begins the formation of oxides of transition metals that are presents in raw materials (Al, Si and Mg), the  $\text{Mg}_2\text{SiO}_4$  and  $\text{AlF}_3$  phase are formed (ICDD 01-074-1683 and ICDD 00-043-0435 respectively). The effect of  $\text{MgO}$  is observed in the formation of  $\alpha$ -alumina and mullite at low temperature (ICDD 01-074-1081 and 98-02-8246 respectively). At 800 °C start the crystallization  $\alpha$ -alumina and mullite, in the beginning the proportion of alumina is bigger than mullite under 1200 °C. At 1200 °C crystalline  $\alpha$ - $\text{Al}_2\text{O}_3$  platelets and some mullite crystals were also found and the increment of temperature serves to dissolution of the  $\alpha$ - $\text{Al}_2\text{O}_3$  to form mullite, and finally at 1400 °C in the diffractogram there is only the presence of crystalline mullite with well-defined planes and the absence of the  $\alpha$ - $\text{Al}_2\text{O}_3$  planes.

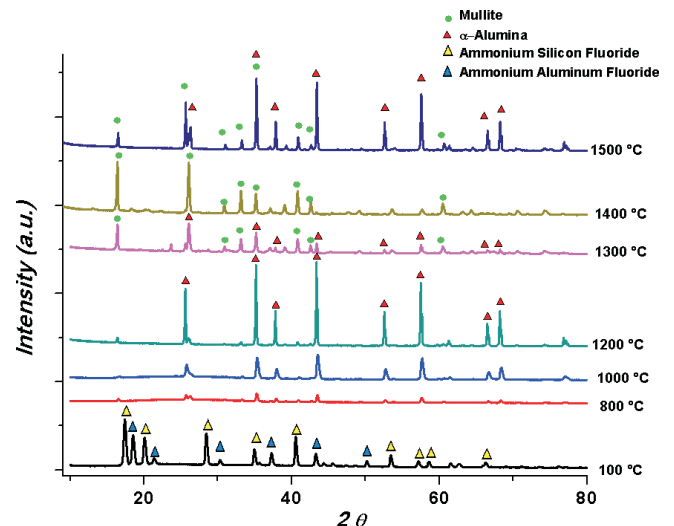


Fig. 2: XRD patterns of experimental sample obtained by Pechini Method, after heat treatment at 100 °C, 800 °C, 1000 °C, 1200 °C, 1300 °C, 1400 °C and 1500 °C.

In order to investigate the stability of mullite the sample is heated to 1500 °C, and it is found that the increase in temperature serves for the decomposition of mullite to form  $\alpha$ -Al<sub>2</sub>O<sub>3</sub>, the results coincide with the literature, where it is reported that the mullite decomposes at high temperature and loses SiO<sub>2</sub> when it is thermally treated in a helium reducing atmosphere between 1650 and 1800 °C<sup>32–37</sup>. In more recent reports it is seen that the mullite decomposes in the range of 1900 to 2000 °C in a graphite furnace without reducing atmosphere<sup>39–45</sup>. Thermodynamically, the decomposition mechanism of mullite must be based on the phase diagram of the SiO<sub>2</sub>-Al<sub>2</sub>O<sub>3</sub> system<sup>1</sup>. Upon heating the mullite will begin phase separation at 1828 °C in  $\alpha$ -alumina and an aluminosilicate liquid, in this case the separation of mullite and alumina is carried out at 1500 °C, demonstrating the role of the precursors used to obtain the refractory phases at a lower temperature.

(c) *Infrared spectroscopy*

Phase evolution upon firing (25–1400 °C) can be systematically followed by IR analysis as shown in Fig. 3 and characteristics bands of the precursors and final phases are shown in Table 1. In the range of 25 to 200 °C a broad band is observed at about 3200 cm<sup>-1</sup>, which is typical of the O-H stretching. The presence of two bands at about 2870 cm<sup>-1</sup>, which corresponds to C-H stretching, and at 1420 cm<sup>-1</sup> due to C-H bending vibration related with the citrate ions. The band ranged about 1780 cm<sup>-1</sup> is reported to agree to the carboxylate anion (COO<sup>-</sup>) stretching mode (a covalent carbonyl bond). The last clear band observed is ranged at about 1680 cm<sup>-1</sup> and can be assigned to the anti-symmetric COO<sup>-</sup> stretching mode for a bridge-type complex, as well as the band over 1120 cm<sup>-1</sup> is related to ester bonds type<sup>4,5,38,39</sup>. Although the IR spectrum at 100 °C presents similar bands as that at 200 °C, the decreasing intensity clearly establishes the gradual loss of water and the citrate and carboxylate groups. It's important to mention the wide band appearing between 500 and 900 cm<sup>-1</sup>. This region corresponds to the vibrational frequencies of coordinated O-Al-O bonds and begins to take importance at relative low temperatures. Up to 400 °C the pyrolysis process continues as it is demonstrated by the strong intensity decreasing of the carboxylate anions and organic chain bands. The typical bands for the carboxylate anions have disappeared at ~400 °C, and only a trace of the carboxylate ions band remains at this temperature. These results sug-

gest that most of the organic chains break down between 300 and 450 °C according with DSC and TGA analysis results.

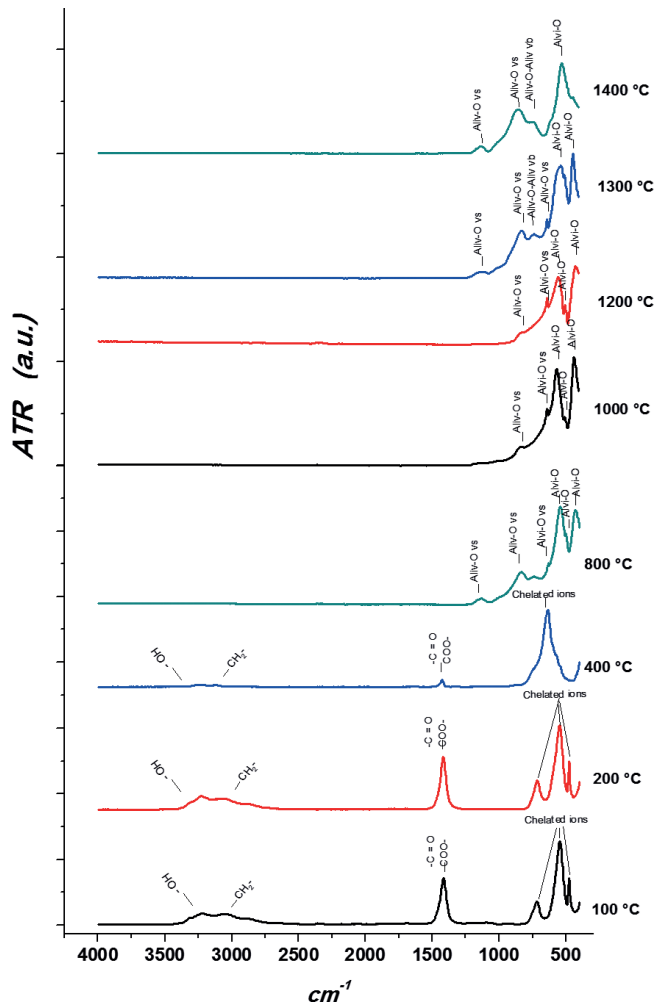


Fig. 3: Infrared spectra of experimental sample obtained by Pechini method, after heat treatment: 100 °C, 200 °C, 400 °C, 800 °C, 1000 °C, 1200 °C, 1300 °C and 1400 °C.

The band ranged at about 500–1100 cm<sup>-1</sup> kept gaining intensity. Characteristic alumina band appear at 400 °C, in the 627 cm<sup>-1</sup> corresponding to the tetrahedral Al<sup>iv</sup>-O vibrations. The wide band, corresponding to the Al-O bonds for  $\alpha$ -Al<sub>2</sub>O<sub>3</sub>, develop in three bands at 622, 545 and 500 cm<sup>-1</sup> as temperature increases up to 800 °C<sup>4,5,37,38</sup>.

Table 1: Band positions in the infrared spectra of porcelain phases.

Structure	Wavenumber (cm <sup>-1</sup> )	Assignment	Structure	Wavenumber (cm <sup>-1</sup> )	Assignment
Mullite	1143	Aliv-O vs	Mullite	827	Aliv-O vs
Mullite	1131	Si-O vs	Mullite	735	Aliv-O-Aliv vb
Mullite	1105	Si-O vs	Mullite	827	Aliv-O vs
Alumina	627	Alvi-O vs	Alumina	545	Alvi-O
Alumina	622	Alvi-O	Alumina	500	Alvi-O

The characteristic mullite bands also appear at 800 °C, for the 1143, 827 and 735  $\text{cm}^{-1}$  spectral region corresponding to the tetrahedral  $\text{Al}^{\text{IV}}\text{-O}$  bands. The Si-O bands appear in the 1131, 1105 and 979  $\text{cm}^{-1}$ . At 1200 °C, the strong and well-defined IR bands observed for Al-O bonding must be explained considering the pure XRD reflections of  $\alpha$ -alumina observed<sup>2,3,18</sup>. The mullite bands show an increasing amount of the mullite phase up to 1300 °C and higher definition of these bands is observed at 1400 °C.

#### (d) Scanning Electron Microscopy

In Fig. 4, the details of the microstructure of the samples that were studied by SEM analysis are exposed. Fig. 4 a)

and 4 b) demonstrations the particles obtained at 800 °C in two different zones of the sample prepared for this analysis, where it can be seen hexagonal platelets of  $\alpha$ -alumina and acicular mullite. In Fig. 4 c) and 4 d) the particles obtained at 1000 °C are shown, in these micrographs a greater amount of acicular mullite is observed, it is important to point out that the morphology of the acicular mullite differs in dimensions with respect to the obtained at 800 °C. According to the results of XRD, an excellent crystallization of the  $\alpha$ -alumina occurs with the temperature increase up to 1200 °C, this can be confirmed by the size of the  $\alpha$ -alumina platelets that were obtained at 1200 °C, which are shown in Fig. 4 e) and 4 f).

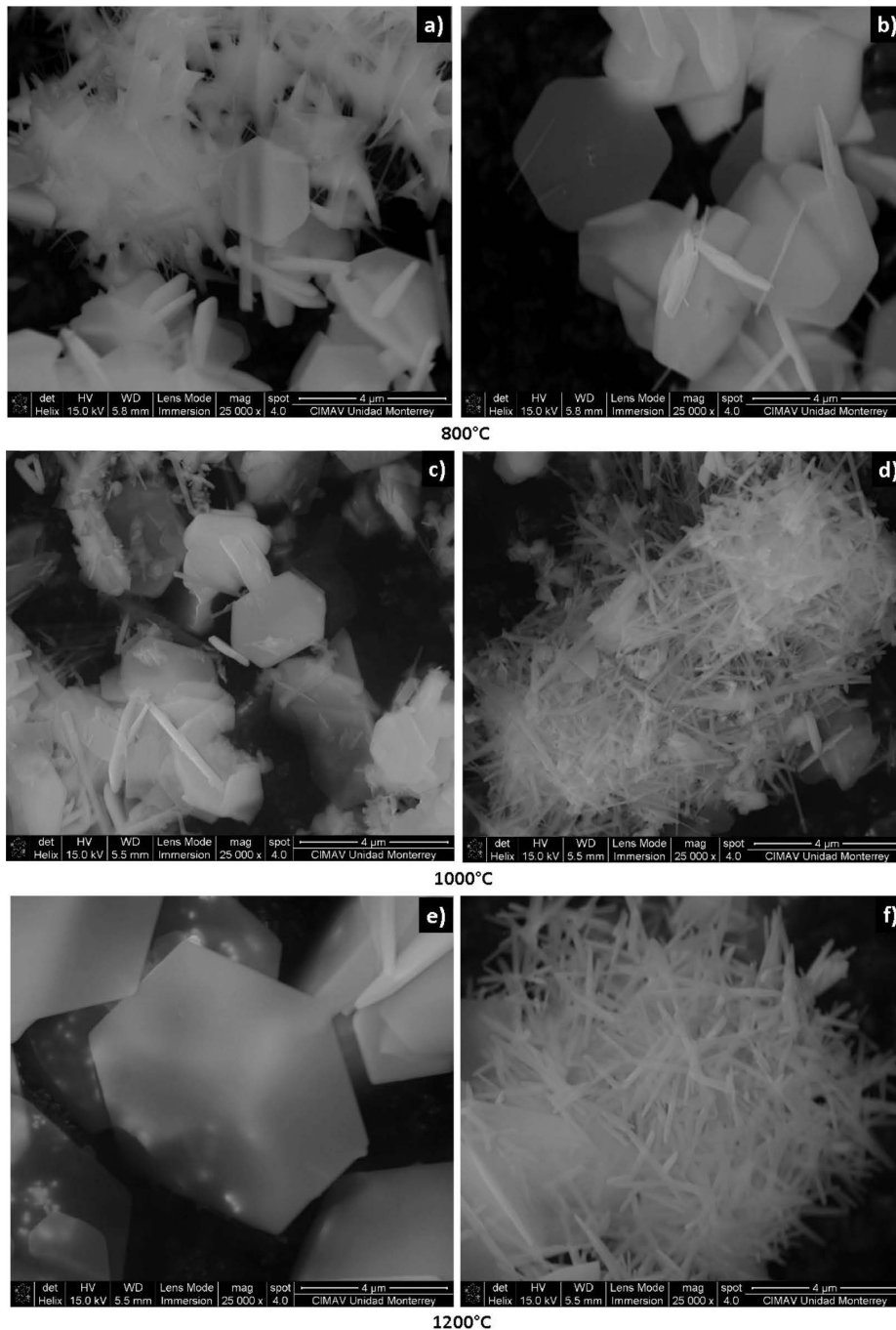


**Fig. 4:** SEM showing mullite and alumina obtained by Pechini method, a) mixture of alumina platelets and acicular mullite formed at 800 °C, b) alumina platelets formed at 800 °C, c) mixture of alumina platelets and acicular mullite formed at 1000 °C, d) acicular mullite formed at 1000 °C e) alumina platelets formed at 1200 °C, f) acicular mullite formed at 1200 °C.

On the other hand, the greater mullitization in acicular form is achieved at a higher temperature (> 1200 °C), in Fig. 4 f) the morphology of the mullite with greater definition and length was observed.

In Fig. 5 a) and 5 b) it can be seen the micrographs of the sample obtained at 1300 °C, where it is observed how the hexagonal  $\alpha$ -alumina platelets were dissolved. On the other hand the acicular mullite increases its length and thickness. In Fig. 5 c) and 5 d) the micrographs of the sample obtained at 1400 °C are shown, in this case no  $\alpha$ -alumina platelets are observed, only the presence of acicular mullite, which can be corroborated with the results of XRD. Finally, in Fig. 5 e) and 5 f), it is observed that the mullite begins to dissolve and again there is a minimum amount of

the presence of  $\alpha$ -alumina platelets. When the temperature increases to 1500 °C, the dissolution of the mullite crystals occurs as seen in the approach of Fig. 5 f), where the crystals lose their edges; this dissolution provides the formation of hexagonal plates corresponding to alpha alumina.

The results of XRD and SEM show the presence of two crystalline phases, mullite needles and  $\alpha$ -alumina platelets. In chemical synthesis processes, such as the sol-gel method, it is possible to obtain the same result. However, the cost of the sol-gel route rises considerably with respect to that proposed in the present work, due to the use of alkoxides as precursors for the synthesis process. In addition to the temperature and time of calcination which are factors that directly affect the increase in costs.

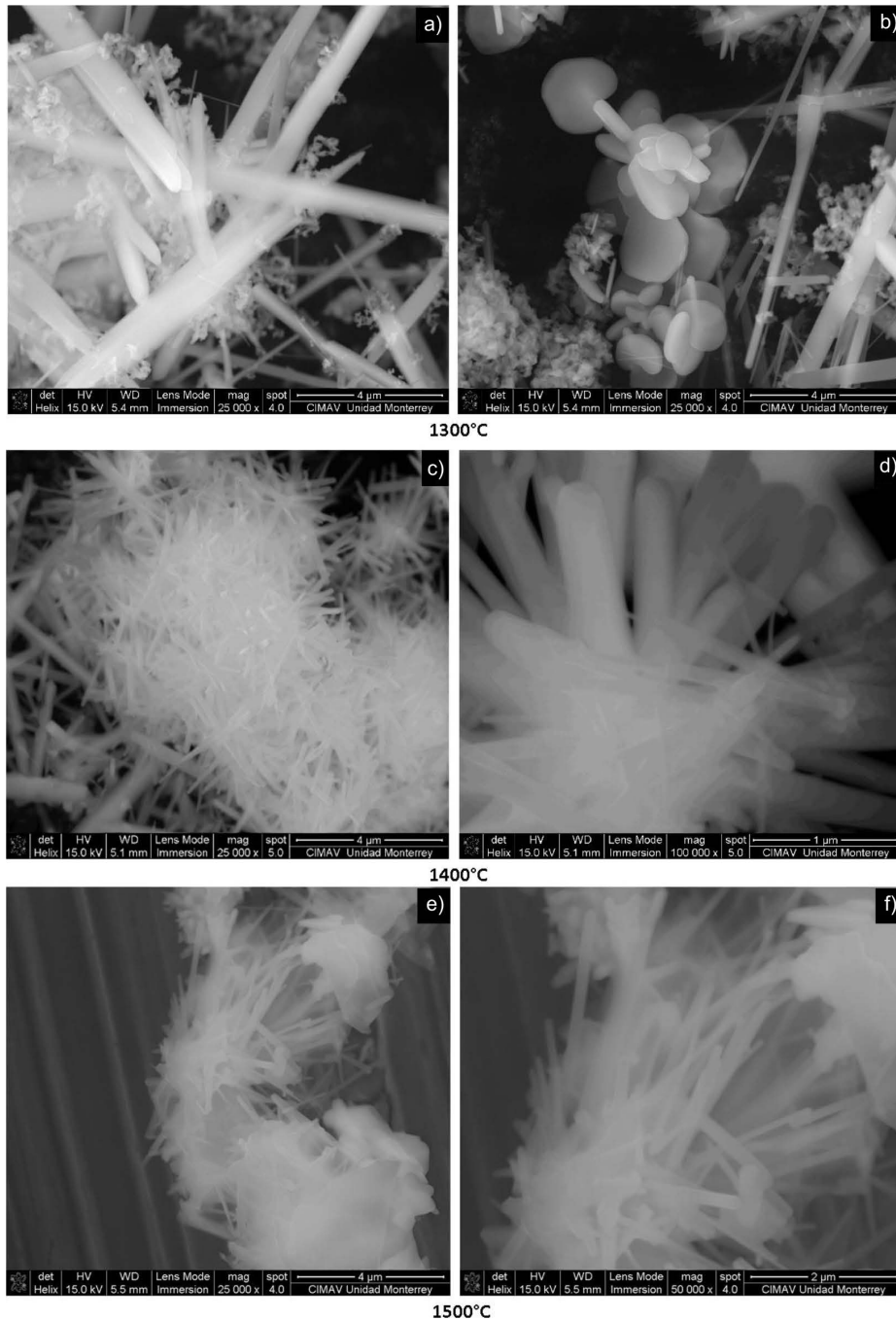


Fig. 5: SEM showing Mullite and alumina obtained by Pechini method a) Acicular Mullite formed at 1300 °C, b) Mixture of alumina platelets and acicular Mullite formed at 1300 °C, c) Acicular Mullite formed at 1400 °C, d) Acicular Mullite and Mullite tertiary formed at 1400 °C, e) Acicular Mullite formed at 1500 °C and f) Acicular Mullite formed at 1500 °C.

The crystalline phases that are obtained by means of this type of synthesis routes, based on chemical routes, such as the sol-gel method and the Pechini method, are found in the solid solution region of the phase diagram of the  $\text{MgO-Al}_2\text{O}_3\text{-SiO}_2$  system<sup>1</sup>. From this diagram, it can also be deduced that the crystalline phases obtained by each of the methods of synthesis will probably maintain their refractory properties up to 1832 °C. According to the diagram of mullite-corundum, if the temperature increases to 1832 °C, it is probable that only alumina is obtained<sup>1</sup>.

## (2) Synthesis of alumina-mullite composite

### (a) Thermal gravimetric Analysis and Differential scanning calorimetry

Fig. 6 shows the result of the TGA and DSC analyzes of the compounds of mullite-corundum-magnesium oxide. In TGA a significant weight loss in a temperature range of 25 °C to 650 °C is seen, weight loss is attributed to water and decomposition of binder. In the range of 650 °C to 1500 °C, a final weight loss of 7% is observed for the formation of alumina and mullite. In the range temperature of 1050 °C to 1350 °C, a weight gain is observed, which is indicative of an oxidation reaction. Finally, in 1300 °C to 1500 °C a slight weight loss is observed due to structural rearrangement of  $\alpha$ - $\text{Al}_2\text{O}_3$  and mullite. Analysis of Differential Scanning Calorimetry presented in Fig. 6, reflecting the decomposition of organic compounds having two endothermic peaks at a temperature of 100 °C and 350 °C, one endothermic band attributed to the formation of  $\alpha$ - $\text{Al}_2\text{O}_3$  and primary mullite, one exothermic peak at 1250 °C corresponding to the crystallization of  $\alpha$ - $\text{Al}_2\text{O}_3$ , and finally, the endothermic peak observed at a temperature of 1350 °C probably represents the dissolution temperature for alumina crystal growth of mullite secondary type III<sup>2,3</sup>, according with XRD and SEM micrographs.

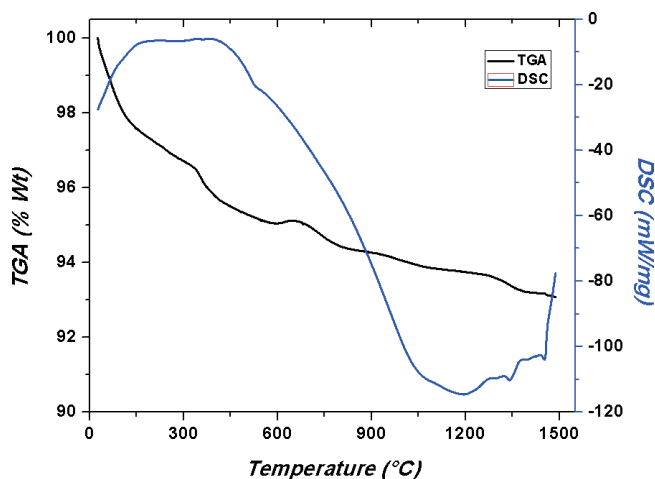


Fig. 6: TGA and DSC curves of composite material sample up to 1500 °C, with a speed of 10 K/min.

### (b) X-Ray Diffraction

The XRD of the fired composite and the corresponding diffraction patterns are shown in Fig. 7. At 1100 °C the crystallization of  $\alpha$ - $\text{Al}_2\text{O}_3$  begins and ends at 1200 °C, crystalline platelets of  $\alpha$ - $\text{Al}_2\text{O}_3$  and some mullite crystals

were also found. The increment of temperature serves to dissolution of the  $\alpha$ - $\text{Al}_2\text{O}_3$  to form mullite at 1300 °C. Finally, at 1400 °C,  $\alpha$ - $\text{Al}_2\text{O}_3$  is present in lower proportion than mullite crystals.

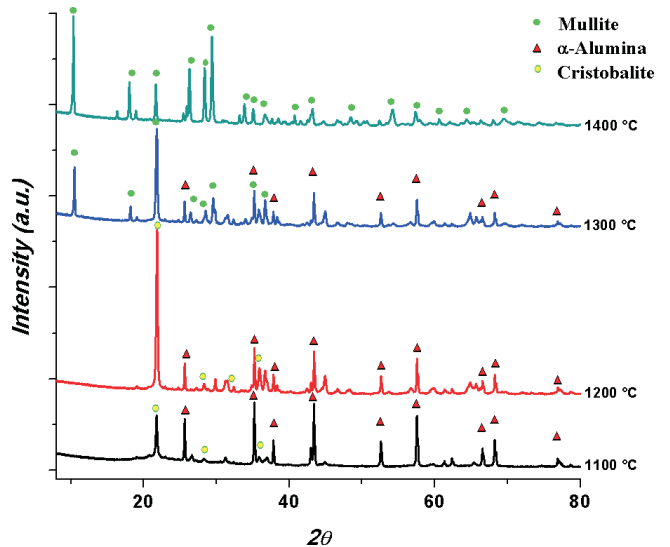


Fig. 7: XRD patterns of composite material sample after heat treatment at 1100 °C, 1200 °C, 1300 °C and 1400 °C.

### (c) Scanning Electron Microscopy

The microstructure of the composite was analyzed by SEM as shown in Fig. 8. The obtained mullite crystals are present in acicular form, whereas, the  $\alpha$ -alumina are recognized by the relicts of hexagonal plates in the micrographs of samples. An excellent crystallization of the  $\alpha$ -alumina occurs with the increment of temperature up to 1200 °C, according the shape of the peaks of the reflections that are presented in the XRD results. On the other hand, the higher mullitization in acicular form is achieved at higher temperature (> 1200 °C). The micrographs show the dissolution of alumina in the range 1200–1400 °C as well as acicular mullite appearance. In the elemental mapping of samples, where one can observe that oxygen, aluminum is uniform throughout the  $\alpha$ -aluminum oxide plates at 800 °C; and oxygen, aluminum and silicon distribution for pure mullite at 1400 °C.

### (d) Results in comparison with other methods

Most of the methods reported in the literature for the synthesis of  $\alpha$ -alumina and Mullite, use chemical synthesis in which alkoxides are involved as precursors (see Table 2). The chemical reactions that are carried out with the alkoxides are more homogeneous, due to the nucleation of small particles that are formed in the reactions that are carried out in the Pechini method.

The small particles allow to obtain lower temperatures in the transformation of crystalline phases. The nature of the precursors can promote the formation of a specific phase. The temperatures for obtaining  $\alpha$ -alumina and mullite vary from 800 to 1800 °C, as can be seen in Table 2.

**Table 2:** Comparison of the variables that have the greatest influence on production costs, for several synthetic methods of  $\alpha$ -alumina and acicular Mullite platelets, reported in the literature and the method reported in this paper.

Authors	Precursors	Method	Temperature (°C)	Time (hrs)	Observations	Reference
Zalapa et al.	Aluminum oxide, silicon oxide and magnesium oxide, hydrofluoric acid, citric acid and propylene glycol	Pechini and sintered	800–1500	2	Formation and dissolution of the platelets of $\alpha$ -alumina and the acicular Mullite, obtained by the Pechini method Phases obtained by means of sinterization of ceramic bodies	This work
Davis et al.	Mullite	ingot prepared by an arc fusion process	1650–1800	0.5–12	Decomposition of the mullite	38
Ribero et al.	Colloidal silica and aluminum hydroxide gel	hydroxigels	1300–1500	4–10	The obtained Mullite crystals present an acicular form, whereas the $\alpha$ -alumina are recognized by their hexagonal plates	40
Su et al.	Ammonia solution, aluminum nitrate, potassium sulfate and polyethylenglycol	Calcining	800–900	2	They obtained a morphology of Single-crystal $\alpha$ -alumina platelets.	7
Reyes et al.	Clay, feldspar and quartz	Slip casting and sintered	1000–1300	2	Acicular Mullite	2
Sathyaseelan et al.	Aluminum nitrate and urea	Combustion synthesis	900–1000	2	Obtained particles of an extremely small grain size, in a range of sizes of 30–50 nm in diameter.	41
Roy et al.	Aluminum nitrate nanohydrate, aluminum isopropoxide, tetra ethyl orthosilicate, iron nitrate, nickel chloride hexahydrate and copper sulfate pentahydrate	Sol-gel Method	1000–1300	2	They obtained particles in a size range of 200 to 500 nm, some hexagonal crystals	42
Nikzad et al.	Glycine, Aluminum nitrate, magnesium nitrate and colloidal silica	Microwave sintering	1200–1400	not available	They obtained particles in a size range of 302 to 478 nm	43
Reyes et al.	Aluminum formate, aluminum metal, formic acid and mercuric chloride	Chemical synthesis	1100 °C	1	Spherical shape granules within 0.1 to 6 $\mu$ m diameter of $\alpha$ -alumina	4

Eventually it is possible to obtain pure phases separately, but in other occasions mixtures of the two phases are obtained. The  $\alpha$ -alumina platelets have been obtained from 800 °C, however, their dissolution temperature is not defined, limiting factor to define a specific application for these particles. On the other hand, the lowest temperature

reported to obtain acicular mullite is 1000 °C. The time of permanence in the crystallization temperature of  $\alpha$ -alumina and mullite during its obtaining, is an important factor that directly affects the production expenses. According to the references reported in Table 2, the permanence time is in a range of 0.5 to 12 hours.



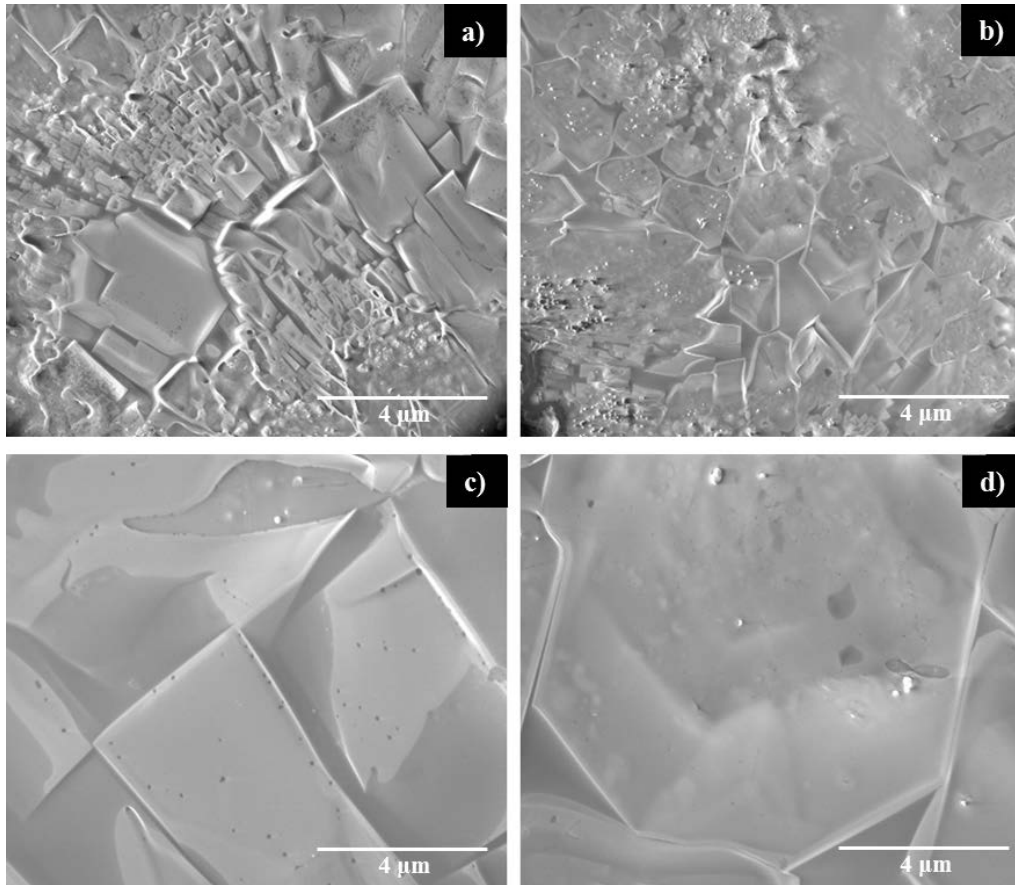


**Fig. 8:** SEM showing mullite and alumina obtained in composite material sample a) and b) crystals of mullite and alumina obtained at 1300 °C; c) and d) crystals of mullite and alumina obtained at 1400 °C.

#### IV. Conclusions

In this article,  $\alpha$ -alumina and mullite are compared, obtained by means of the Pechini method and by sintering oxides. Using the Pechini method, mullite needles and plates of  $\alpha$ -aluminum oxide at 800 °C and pure mullite at 1400 °C were obtained using a dwell time of 2 hours. These results require a lower amount of energy, compared to the references cited in Table 2. The results obtained by the sintering of oxides, taking into account that the precursor oxides are amorphous and of submicron size, it was necessary to use 200 °C more in the sintering temperatures for the obtaining of the phases, in comparison with the temperatures used in the Pechini method. This research demonstrates the impotence of the precursors used to obtain the phases of mullite and alumina at a temperature lower than 1800 °C. The Pechini method presented in this research is a good alternative for obtaining  $\alpha$ -alumina platelets and acicular mullite, with special characteristics such as high purity, homogeneity and crystallinity. With respect to the above, it is concluded that the Pechini method used in the present research is efficient in terms of energy consumption in comparison with the methods of the references cited in Table 2.

#### Data Availability

The data used to support the findings of this study are available from the corresponding author upon request.

#### Conflict of Interest

The authors declare that they have no conflict of interest.

#### Acknowledgments

The authors gratefully acknowledge the financial support by CONACYT, PRODEP, Universidad Autónoma de Ciudad Juárez and Centro de Investigación en Materiales Avanzados - Monterrey, for allowing the development of this project to be done satisfactorily in a timely manner.

#### References

- 1 Stolyarova, V. L., Lopatin, S. I., Fabrichnaya, O. B.: Thermodynamic Properties of silicate glasses and melts: VIII. System MgO-Al<sub>2</sub>O<sub>3</sub>-SiO<sub>2</sub>, Russian J. Gen. Chem., **81**, 2051–2061, (2011).
- 2 Reyes-López, S. Y., Rodríguez-Serrato, J., Sugita-Sueyoshi, S.: Microstructural characterization of sanitaryware, the relationship spinel and Mullite, J. Ceram. Proc. Res., **14**, 492–497, (2013).
- 3 Reyes-López, S. Y., Rodríguez-Serrato, J.: Microstructural characterization of sanitaryware by infrared and Raman spectroscopy, the role of vitreous matrix on properties, J. Ceram. Proc. R., **16**, 162–168, (2015).
- 4 Reyes-López, S. Y., Rodríguez-Serrato, J., Sugita-Sueyoshi, S.: Low-temperature formation of alpha alumina powders via metal organic synthesis. AZO J. of Mat., **2**, 1–9, (2006).
- 5 Reyes-López, S. Y., Saucedo-Acuña, R., López-Juárez, R. & Rodríguez-Serrato, J.: Analysis of the phase transformation of aluminum formate Al(O<sub>2</sub>CH)<sub>3</sub> to  $\alpha$ -alumina by Raman and infrared spectroscopy, J. Ceram. Proc. R., **14**, 627–631, (2013).
- 6 Hernández, M. T. & González, M.: Synthesis of resins as alpha-alumina precursors by the Pechini method using microwave and infrared heating, J.E. Ceram. Soc., **22**, 2861–2868, (2002).

- 7 Su, X., Li, J.: Low temperature synthesis of single-crystal alpha alumina platelets by calcining bayerite and potassium sulfate, *J. Mater. Sci. Tech.*, **27**, 1011–1015, (2011).
- 8 Hill, R.F., Danzer, R., Paine, R.T.: Synthesis of aluminium oxide platelets, *J. Am. Ceram. Soc.*, **84**, 514 (2001).
- 9 Miao, X., Sorrell, C.C.: Alumina Platelets from Topaz-zirconia Mixtures, *J. Mater. Sci. Lett.*, **17**, 2087, (1998).
- 10 Hashimoto, S., Yamaguchi, A.: Synthesis of  $\alpha$ -Al<sub>2</sub>O<sub>3</sub> platelets using sodium sulfate flux, *J. Mater. Res.*, **14**, 4667, (1999).
- 11 Park, H.C., Kim, S.W., Lee, S.G., Kim, J.K., Hong, S.S., Lee, G.D., Park S.S.: Synthesis of  $\alpha$ -alumina platelets using flux method in 2.45 GHz microwave field, *Mater. Sci. Eng. A*, **363**, 330–334, (2003).
- 12 Wu, Y., Choy, K.L., Hench, L.L.: Preparation of  $\alpha$ -Alumina Platelets by Laser Scanning, *J. Am. Ceram. Soc.*, **87**, 1606–1608, (2004).
- 13 Wei, M., Zhi, D., Choy, K.L.: Novel synthesis of  $\alpha$ -alumina hexagonal nanoplatelets using electrostatic spray assisted chemical vapour deposition, *Nanotechnology*, **17**, 181–184, (2006).
- 14 Galassi, C., Roncari, E., Bassarello, C., Lapasin, R.: Influence of Magnesia Addition on the Rheological Properties of Mullite Suspensions, *J. Am. Ceram. Soc.*, **82**, 3453–3458, (1999).
- 15 Amutharani, D., Gnanam, F.D.: Low temperature pressureless sintering of sol-gel derived Mullite, *Mater. Sci. Eng. A*, **264A**, 254–261, (1999).
- 16 Chaudhuri, S.P., Partra, S.K.: Preparation and Characterization of Transition Metal Ion Doped Mullite, *Trans. Br. Ceram. Soc.*, **96**, 105–111, (1997).
- 17 Somiya, S., Yoshimura, M., Suzuki, M., Yanaguchi, T.: Ceramic transaction: Mullite and mullite matrix composites, *Am. Ceram. Soc.*, **6**, 287–317, (1990).
- 18 Gopi Chandran, R., Chandrashekar, B. K., Ganguly, C., Patil, K. C.: Sintering and microstructural investigations on combustion processed Mullite, *J. Eur. Ceram. Soc.*, **16**, 843–849, (1996).
- 19 Hirata, Y., Aksay, I. A., Hori, S., Kaji, H.: Ceramic transaction: Mullite and mullite matrix composites, *Am. Ceram. Soc.*, **6**, 287–317; (1990).
- 20 Lee, W.E., Rainforth, W.M.: Ceramic microstructures: Property control by processing, **1**, 299–311, (1994).
- 21 Viswabaskaran, V., Gnanam, F.D., Balasubramanian, M.: Mullitisation Behaviour of Calcined Clay-Alumina Mixtures, *Ceram. Int.*, **29**, 561–571, (2003).
- 22 Sainz, M. A., Serrano, F.J., Bastida, J., Caballero, A.: Microstructural evolution and growth of crystallite size of mullite during thermal transformation of kyanite, *J. Eur. Ceram. Soc.*, **17**, 1277–1284, (1997).
- 23 Ismail, M. G. M. U., Tsunatori, H., Nakai, Z.: Preparation of MgO-doped mullite by sol-gel method, powder characteristics and sintering, *J. Mater. Sci.*, **25**, 2619–2625, (1990).
- 24 Shin, H., Kim, C., Chang, S.: Mullitization from a multicomponent oxide system in the temperature range 1200–1500 °C, *J. Am. Ceram. Soc.*, **83**, 1237–40, (2000).
- 25 Viswabaskaran, V., Gnanam, D., Balasubramanian, M.: Mullite from clay-reactive alumina for insulating substrate application, *Appl. Clay Sci.*, **25**, 29–35, (2004).
- 26 Doni, D., Amutha, D., Benny, D., Ma, J., Ohji, T.: Pulse electric current sintering and microstructure of industrial mullite in the presence of sintering aids, *Ceram. Int.*, **30**, 539–543, (2004).
- 27 Sacks, M. D., Lee, H., Pask, J. A.: Ceramic transaction: Mullite and mullite composites, *Am. Ceram. Soc.*, **6**, 167–208, (1990).
- 28 Viswabaskaran, V., Gnanam, F.D., Balasubramanian, M.: Effect of MgO, Y<sub>2</sub>O<sub>3</sub> and boehmite additives on the sintering behavior of mullite formed from kaolinite-reactive alumina, *J. Mater. Process. Technol.*, **142**, 275–281, (2003).
- 29 Cesário, M. R., Macedo, M. A., Oliveira, R. M. P. B., Pimentel, P.M., Moreira, R. L., Melo, D. M. A., The synthesis, thermal stability, crystal structure and spectroscopic study of La<sub>0.80</sub>Sr<sub>0.20</sub>MnO<sub>3</sub> powder obtained by the modified Pechini's method, *J. Ceram. Process. Res.*, **12**, 102–105 (2011).
- 30 Chakraborty, A.K., Ghosh, D.K.: Reexamination of the Kaolinite-to-Mullite Reaction Series, *J. Am. Ceram. Soc.*, **61**, 170–173, (1978).
- 31 Rezaie, H. R., Rainforth, W. M., Lee, W. E.: Mullite evolution in ceramics derived from kaolinite, kaolinite with added  $\alpha$ -alumina, and sol-gel precursors. *Trans. Br. Ceram. Soc.*, **96**, 181–187, (1997).
- 32 Viswabaskaran, V., Gnanam, F. D., Balasubramanian, M.: Mullitisation behavior of South Indian Clay, *Ceram. Int.*, **28**, 557–564, (2002).
- 33 Montanaro, L., Perrot, C., Esnouf, C., Thollet, G., Fantozzi, G., Negro, A.: Sintering of Industrial Mullites in the Presence of Magnesia as a Sintering Aid, *J. Am. Ceram. Soc.*, **83**, 189–196, (2000).
- 34 Amutha Rani, D., Doni Jayaseelan D., Gnanam, F. D.: Densification behavior and microstructure of gel-derived phase-pure, Mullite in the presence of sinter additives, *J. Europ. Ceram. Soc.*, **21**, 2253–2257, (2001).
- 35 Hong, S.H., Cermignani, W., Messing, G. L.: Anisotropic grain growth in seeded and B<sub>2</sub>O<sub>3</sub>-doped diphasic Mullite gels, *J. Europ. Ceram. Soc.*, **16**, 133–141, (1996).
- 36 Hong, S.H., Messing, G. L.: Anisotropic grain growth in dysphasic-gel-derived titania-doped Mullite, *J. Am. Ceram. Soc.*, **81**, 1269–1277, (1998).
- 37 Mechnich, P., Schmucker, M., Schneider, H.: Reaction sequence and microstructural development of CeO<sub>2</sub>-doped reaction-bonded Mullite, *J. Am. Ceram. Soc.*, **82**, 2517–2522, (1999).
- 38 Roque-Ruiz, J.H., Cabrera-Ontiveros, E.A., González-García, G., Reyes-López, S. Y.: Thermal degradation of aluminum formate sol-gel; synthesis of  $\alpha$ -alumina and characterization by <sup>1</sup>H, <sup>13</sup>C and <sup>27</sup>Al MAS NMR and XRD spectroscopy. *Results in physics*, **6**, 1096–1102, (2016).
- 39 Roque-Ruiz, J.H., Reyes-López, S. Y.: Synthesis of  $\alpha$ -Al<sub>2</sub>O<sub>3</sub> nanopowders at low temperature from aluminum formate by combustion process. *J. Material Sci Eng* 2016, **6**, 305; DOI: 10.4172/2169-0022.1000305.
- 40 Xiao, Z., Brian, S.: Mullite Decomposition Kinetics and Melt Stabilization in the Temperature Range 1900–2000 °C, *J. Am. Ceram. Soc.*, **83**, 761–767, (2000).
- 41 Davis, R. F., Aksay, I. A., Pask, J. A.: Decomposition of Mullite, *J. Am. Ceram. Soc.*, **55**, 98–101 (1972).
- 42 Liu, K. C., Thomas, G.: Mullitisation behaviour of calcined clay-alumina mixtures *J. Am. Ceram. Soc.*, **77**, 545–552, (1994).
- 43 Ribero, D., Restrepo, R., Paucar, C., García, C.: Highly refractory mullite obtained through the route of hydroxyhydrogels, *J. Mat. Proc. Tech.*, **209**, 986–990, (2009).
- 44 Sathyaseelan, B., Baskaran, I., Sivakumar, K.: Phase Transition Behavior of Nanocrystalline Al<sub>2</sub>O<sub>3</sub> Powders, *S. Nanoscience L.*, **3**, 69–74, (2013).
- 45 Roy, D., Bagchi, B., Bhattacharya, A., Das, S., Nandy, P.: Microwave sintering of mullite-cordierite precursors prepared from solution combustion synthesis, *Int. J. Appl. Ceram. Technol.*, **11**, 1054–1060, (2014).
- 46 Nikzada, L., Ghofrani, S., Majidian, H., Ebadzadeh, T.: Microwave sintering of mullite-cordierite precursors prepared from solution combustion synthesis, *Ceram. Int.* **41**, 9392–9398, (2015).